

Received March 21, 2022, accepted April 15, 2022, date of publication April 20, 2022, date of current version May 4, 2022.

Digital Object Identifier 10.1109/ACCESS.2022.3168971

Optimization and Transient Analysis of Distributed Asynchronous Condenser

ZHIPENG LIU¹, HAIBING QI¹, MINGYU XU¹, XINGYUAN JIANG², AND YANLING LV¹

¹Electric Power Research Institute, State Grid Heilongjiang Electric Power Company Ltd., Harbin 150030, China

²School of Electric and Engineering, Harbin University of Science and Technology, Harbin 150080, China

Corresponding author: Yanling Lv (yanling0828@163.com)

This work was supported in part by the 2021 Science and Technology Project of State Grid Heilongjiang Electric Power Company Ltd.,

“Research on new asynchronous condenser to improve the stability of high penetration renewable energy power grid” under Grant 5224372003a.


ABSTRACT After the high proportion of new energy is connected, the decrease of the proportion of synchronous machine in power system will cause a series of stability hazards, such as the lack of inertia. The distributed asynchronous condenser provides a solution for the above problems because of its high controllability, high inertia and high phase advance ability. In this paper, the performance parameters of the distributed asynchronous condenser are analyzed to further optimize its structure. At the same time, the advantages and disadvantages of different excitation schemes are compared and analyzed, and the best scheme is selected; Secondly, a multi physical domain model is established to analyze the magnetic field distribution in steady-state operation and verify the error between the design value and the simulation value; Finally, the transient characteristics of distributed asynchronous condenser under different fault types and different fault parameters are analyzed. Through the above research, this paper verifies that the distributed asynchronous condenser plays the role of reactive power support and voltage regulation on the stability of new energy system.

INDEX TERMS Design optimization, distributed power generation, electromagnetic analysis, electromagnetic transients.

I. INTRODUCTION

In recent years, the installed capacity of wind power in China has increased day by day, and its total capacity has reached 41% of the global installed capacity, which is far more than that of large wind power countries such as the United States and Brazil. Under the goal of “double carbon”, high proportion of new energy and high proportion of power electronic devices are the biggest characteristics of the new power system. The emergence of the new power system is bound to have a series of power grid stability problems [1]–[3].

At present, the proportion of new energy power generation in the new power system is higher and higher, but with the increase of the proportion of new energy and the decrease of the proportion of synchronous machine, the ability of power system to deal with frequency modulation and power oscillation is also greatly reduced. Although the wind turbine of new energy generation can increase its stability and immunity by decoupling with frequency, droop control, improving droop

The associate editor coordinating the review of this manuscript and approving it for publication was Bin Zhou .

control, integrated inertia control and other control modules, the rotor kinetic energy that can be used by variable-speed wind turbine is still very low, and the problem of low inertia of the system is still obvious [4]–[6]. Virtual synchronous generator technology (VSG) is a virtual system with synchronous generator characteristics realized by controller. This technology introduces the inertia and primary frequency modulation characteristics of synchronous generator into the rotor equation and adds them to the control of inverter to make it have similar response characteristics of synchronous generator [7], [8]. Although the frequency modulation effect of VSG technology is similar to that of integrated inertial control as a whole, it cannot support the voltage of microgrid and realize the island operation of microgrid [9]–[12]. Some researchers have proposed to use the energy storage system with wind power or photovoltaic to realize the voltage support and frequency regulation of the system, but the equivalent kinetic energy provided by the energy storage unit is still insufficient to compensate the inertia of the wind power plant [13].

After a large number of new energy sources are connected to the system, the synchronous condenser, as the reactive

power compensation equipment in the system, effectively adjusts the stability in the new energy system with its own advantages of high inertia and excellent voltage regulation ability. For example, two 300Mvar synchronous condensers put into use in Newfoundland, Canada, have an inertia time constant of up to 7.84s [14]. At the same time, since the moment of inertia determines the initial frequency deviation and further determines the resistance of new energy power generation to disturbance in the system, the frequency support ability in the new power system can be effectively enhanced by optimizing the structure of the synchronous condenser to increase its inertia [15], [16]. However, with the increase of the proportion of new energy power generation, the advantages and disadvantages of centralized configuration and distributed configuration of condenser have attracted the attention of some scholars. Some studies show that the access of distributed condenser with optimized algorithm can reduce the total capacity of condenser required by the system by nearly 10%. In 2021, Qinghai, China, put into operation the first 50Mvar distributed salient pole condenser in China, which marks the official launch of the “Security Guard” of new energy transmission [17], [18]. Asynchronous motor, also known as double shaft excitation motor, was first proposed by German engineer Tuxen E in 1935. Until the 1960s, the former Soviet Union first installed two 50MVA asynchronous hydro generators in Ivofošk Hydropower station, which can realize the trial operation of variable speed constant frequency power generation. Then, in the 1990s, Hitachi and Toshiba began to apply symmetrical three-phase excitation to the rotor. Compared with the traditional motor, the asynchronous motor can realize the independent adjustment of active power, reactive power and speed, and can still operate stably and realize the function of variable speed and constant frequency during deep phase advance operation [19]. However, until the end of last century, both in theoretical analysis and practical application, asynchronous technology was only applied to generators and motors, and did not expand outward. Until 2003, Professor Ferreira of the Federal University of Rio de Janeiro in Brazil and other talents proposed a variable-speed adjustable condenser. The research shows that this adjustable condenser can provide a small amount of active power to the system in a short time [20]. However, due to the rapid development of power electronics technology and the large capacity of condenser, there has been no relevant research since then. Until recent years, with the rise of new energy power generation, the rise of distributed condenser began to make it possible to realize the asynchronization of condenser. In this paper, a new asynchronous condenser is proposed, and the distributed asynchronous condenser is designed and optimized for the purpose of increasing the inertia of the condenser. It breaks through the structural constraints and excitation strategy of the traditional salient pole condenser, and looks for an AC excitation scheme suitable for the distributed asynchronous condenser. At the same time, the distributed asynchronous condenser can realize slip conversion, provide reactive power

to the system during synchronous operation, and the conversion process during asynchronous operation can transmit equivalent active power to the system to participate in primary frequency modulation. This paper verifies the equivalent inertia and energy output provided by it in the new energy power generation system, and analyzes the electromagnetic parameters of the distributed asynchronous condenser.

Firstly, this paper analyzes the working principle of the distributed asynchronous condenser and optimizes its performance parameters. Then, starting from the excitation structure, this paper optimizes the excitation structure of the distributed asynchronous condenser in the synchronous state, analyzes and compares the advantages and disadvantages of different excitation schemes, determines the best excitation scheme, and analyzes the electromagnetic characteristics of the excitation scheme. Finally, the transient characteristics of distributed asynchronous condenser under various working conditions are analyzed by establishing a multi physical domain model. It provides a theoretical reference for the safe and stable operation of the follow-up new power system

II. ONTOLOGY OPTIMIZATION

Some pre parameters involved in this section have been calculated and verified. Because the process is basic but cumbersome, it will not be repeated here. This section will take a parameter as an example to introduce the optimization process of distributed asynchronous condenser.

In the process of optimizing the electromagnetic parameters or performance parameters of motor, it is necessary to reasonably select the optimization scheme [21]–[24]. The main reactance and leakage reactance are the most basic and important parameters in the motor performance parameters. Their size directly determines the dynamic performance of the distributed asynchronous condenser. Next, take the main reactance as an example to analyze the ontology optimization process. The calculation formula of the main reactance is shown in equation (1).

$$X_m = 4f\mu_0 \frac{m N^2 K_{dp}^2}{\pi p} l \frac{\tau}{\delta} \quad (1)$$

It can be clearly seen from equation (1) that the fixed parameters such as frequency f , phase number m and vacuum permeability μ_0 are removed as well as fixed values, the polar logarithm p , the winding turns N and the polar distance of the condenser τ are calculated. It is determined in the design process of the main parameters of the condenser (motor rated parameters, inner and outer diameter of iron core, etc.). If adjusted, it will affect a very cumbersome and complex calculation process, so these parameters will not be optimized in general. The variation of optimization range of winding coefficient K_{dp} is very small and can generally be ignored. Therefore, it can be preliminarily determined that the main influencing parameter of reactance is air gap length δ and effective length of iron core l . Its influences are shown in Figure 1.

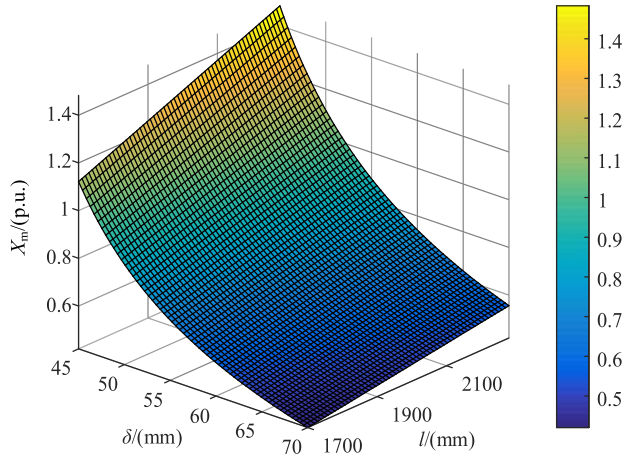


FIGURE 1. The influence of different air gaps and calculated lengths on the main reactance.

It can be clearly seen from Figure 1 that when other parameters are fixed or slightly changed, the air gap length δ and the change of the calculated length l of the iron core will indeed affect the change of the main reactance parameters to a great extent. The optimization range can reach 0.4-1.5, but it is not the extreme point or the best advantage of this optimization. Many other correlation formulas should be referred to.

$$\lambda = \frac{l_{ef}}{\tau} \tag{2}$$

$$J = \frac{\pi}{2} \rho l (r_1^2 + r_2^2) r_2^2 \tag{3}$$

where: λ is the main dimension ratio, J is the moment of inertia, r_1 and r_2 are the outer diameter of the rotor and the outer diameter of the shaft, respectively.

It can be seen from Figure 1 that with the change of the calculated length of the machine body, the change range of the main reactance is not very large. At the same time, it can be seen from equations (2) and (3) that the size of the moment of inertia depends on the calculated length of the iron core and the outer diameter of the rotor. When the size of the motor stator remains unchanged, the outer diameter of the rotor directly determines the length of the air gap, The changes of the above two parameters have a great impact on the moment of inertia. Therefore, in the process of optimizing the main reactance, in order to reduce the impact on the moment of inertia or other important parameters as much as possible, the air gap length δ is selected here instead of the effective length of the iron core l , it is the main optimization parameter of the main reactance. The same optimization process can be applied to the selection of other electromagnetic parameters or parameters, which will not be repeated here.

The same optimization process can be applied to the selection of other electromagnetic parameters or performance parameters. The specific optimization process is shown in Figure 2. The electromagnetic parameters and performance parameters of optimization factors are considered in the process.

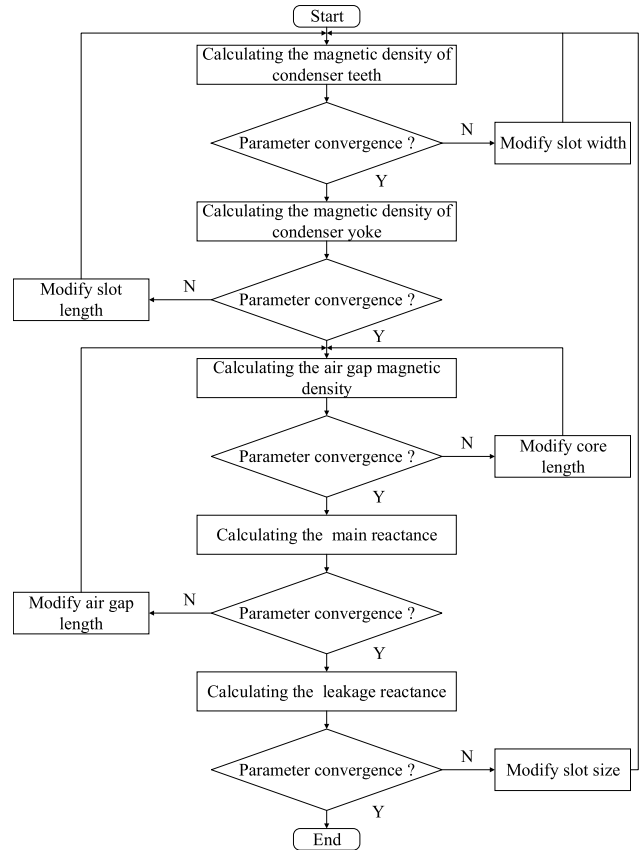


FIGURE 2. Conceptual diagrams of different scenarios.

III. EXCITATION OPTIMIZATION

The distributed asynchronous condenser mentioned in this paper adopts three-phase AC excitation during asynchronous operation, so its rotor structure selects the hidden pole three-phase winding structure. At the same time, in order to reduce the high-order harmonics caused by AC excitation, this paper selects the double-layer winding mode with pitch of 25 according to the number of rotor slots and winding turns. This structural design can meet the high efficiency of the motor, and there can be more selectivity in the grouping of rotor windings. In this paper, five representative schemes are selected for comparative analysis. Their specific numbers and structural differences are shown in Table 1. The five schemes shown in Table 2 have obvious differences in structure and winding arrangement, and each has its advantages and disadvantages, as shown in Figure 3.

As shown in Figure 3, scheme A adopts single-phase winding for excitation. Although the winding utilization is low and its excitation current rating is relatively large, it has good potential in terms of control and can be matched with more flexible control methods. Schemes B and C have high winding utilization. The difference is that Schemes C adopts the original grouping of two-phase excitation windings, In scheme B, the excitation windings are grouped again. Despite the complexity of manufacturing and control, their spatial distribution is uniform. Scheme D and E correspond to

TABLE 1. Five excitation schemes for synchronous operation.

Schemes	Characteristic	Winding utilization	Grade
Scheme A	Single phase order of magnitude double winding	33.3%	a)
Scheme B	Two phase order of magnitude single winding	80.0%	b)
Scheme C	Two phase order of magnitude double winding	66.6%	c)
Scheme D	Three phase order of magnitude double winding	100%	d)
Scheme E	Three phase order of magnitude single winding	100%	e)

TABLE 2. Air gap magnetic density and harmonic distribution.

Schemes	B1/T	B3/T	B5/T	B7/T	THD/%
Scheme A	0.856	0.14	0.014	0.006	16.52
Scheme B	0.962	0.019	0.009	0.007	2.30
Scheme C	0.826	0.012	0.01	0.005	2.04
Scheme D	0.925	0.051	0.003	0.004	5.58
Scheme E	0.907	0.5	0.002	0.004	5.57

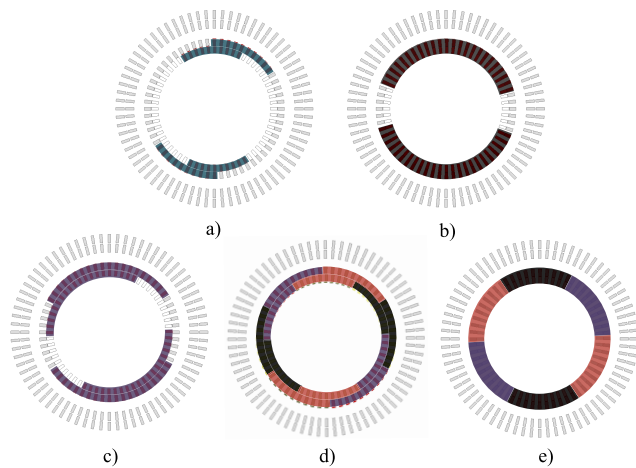


FIGURE 3. Conceptual diagrams of different scenarios.

double-layer stacked windings and single-layer windings respectively. The main difference between them is that the spatial excitation distribution of windings is different. In the above scheme, the winding groups corresponding to the electromagnetic performance of each scheme, the five structures

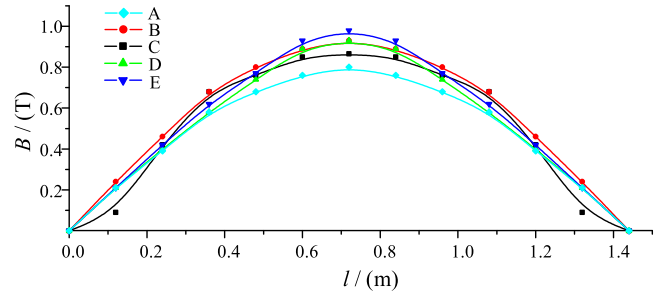


FIGURE 4. Comparison of air gap magnetic density under five schemes.

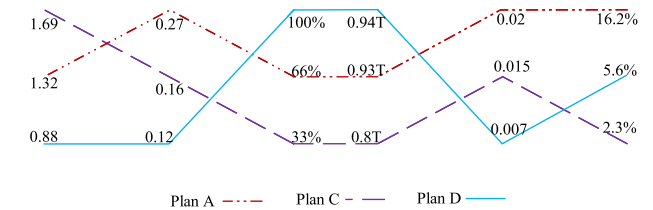


FIGURE 5. Simplified analytic hierarchy process comparison results.

are simulated and analyzed in this paper. In order to facilitate the analysis, the following assumptions are made:

1. Ignore the differences in excitation control methods of different schemes.

2. Ignore the economic cost of motor operation.

Since the air gap magnetic density determines the operating characteristics of the condenser, this paper uses the time-step finite element method to simulate and analyze it. Finally, the air gap magnetic density results of each scheme are shown in Figure 4.

It can be seen from the figure that for a pair of pole motor optimized in this paper, only the data on the semicircle circumference need to be taken for analysis. Moreover, it can be seen from the figure that the harmonic distribution of each scheme is also different, and the maximum air gap magnetic density can reach more than 0.95T. In this paper, the air gap magnetic density harmonics under five schemes are calculated, and the results are shown in Table 2. It can be seen from the Table 2 that the total harmonic distortion rates are 16.52%, 2.3%, 2.04%, 5.58% and 5.57% respectively, which are generally divided into three regions. It can be seen that scheme B and E have no particularly obvious advantages over scheme C and D. This shows that scheme B and E do not show their advantages in the maximum fundamental wave of air gap under the same air gap magnetic density distortion rate, even scheme B has the largest air gap magnetic density, and scheme E and D do not have much difference in electromagnetic performance.

In order to get more obvious experimental results, considering the control and manufacturing difficulties of winding regrouping in the actual operation of the motor, this paper selects three of the five schemes, namely scheme A, scheme C and D, and makes a data weighted comparison by using the simplified analytic hierarchy process. The final result is shown in Figure 5.

TABLE 3. Analytic hierarchy process evaluation results.

Hierarchical sub goal	Scheme A	Scheme C	Scheme D
Synchronous reactance	4.56	0	10.0
Leakage reactance	0	7.33	10.0
Material utilization	5.00	0	10.0
Maximum air gap magnetic density	0.70	10	0
Fifth and seventh harmonics	0	3.84	10
Total harmonic distortion rate	0	10	7.62
Weighted sum	10.26	31.17	47.62

According to the different parameters (from left to right are synchronous reactance, leakage reactance, material utilization, maximum air gap flux density, fifth and seventh harmonic values and THD) in Figure 5, the simplified analytic hierarchy process is used for selection. In order to make the final weighted score as reasonable as possible, this paper uses the variable range half division ratio weighting method to ensure that the worst and optimal parameters correspond to the upper and lower limits respectively. The final evaluation results are shown in Table 3.

It can be seen from the Table 3 that the final weighted sum of scheme D is the largest, so scheme D can be preliminarily selected as the synchronous operation excitation mode of distributed asynchronous condenser.

In this mode, it has better performance parameters and greater material utilization, and it can be preliminarily determined that it has better transient performance and economic advantages.

IV. STRUCTURAL OPTIMIZATION AND VERIFICATION

In order to verify the steady-state operation of the distributed asynchronous condenser and its system, this paper analyzes it through the joint simulation of multi physical domain. The system wiring is shown in Figure 6 and the simulation wiring diagram is shown in Figure 7.

The system consists of distributed asynchronous condenser and its excitation control system, transmission line, wind power generation equivalent system and infinite power system. In the system, the voltage level of the transmission line is 35kV, and the transformer transformation ratio at the outgoing line of the wind power generation system is 690V/10.5kV/35kV. In the simulation results, taking the magnetic field distribution diagram of the distributed

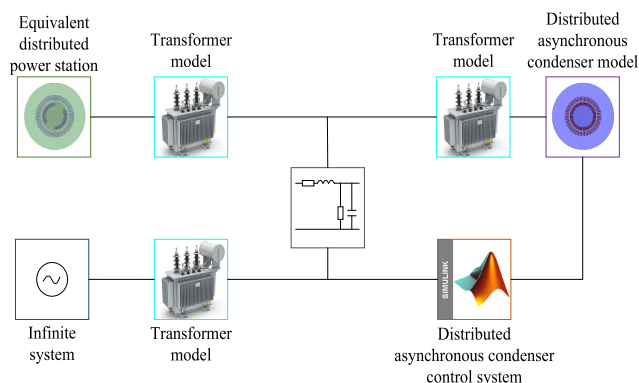


FIGURE 6. Diagram of system wiring.

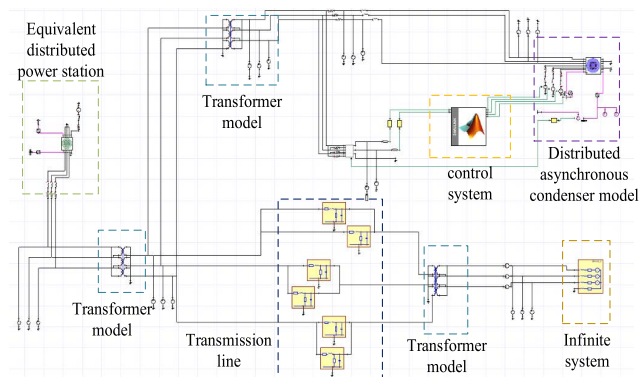


FIGURE 7. Simulation wiring diagram.

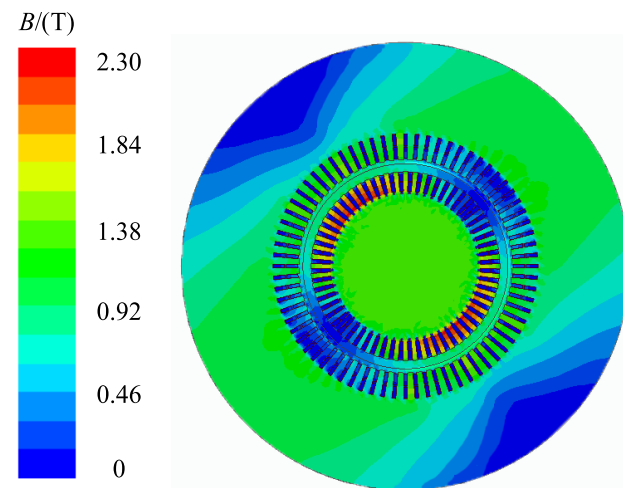


FIGURE 8. Magnetic field distribution diagram during stable operation.

asynchronous condenser after all equipment are in steady-state operation, as shown in Figure 8.

It can be seen from the magnetic density distribution diagram on the right that the maximum magnetic density of the motor is 2.15 T, which is located between the rotor teeth, and the maximum magnetic density of the stator teeth is 1.52 T. In order to more intuitively see the error between the simulation value and the design value, the data in Table 3 listed in this paper are the comparison between the simulation value and the design value.

TABLE 4. Comparison of simulation value and design value.

	Design value /T	Simulation value /T	Error /%
Maximum magnetic density of rotor teeth	2.11	2.15	1.42
Maximum magnetic density of rotor yoke	1.61	1.53	4.96
Maximum magnetic density of stator teeth	1.58	1.52	3.79
Maximum magnetic density of stator yoke	1.51	1.48	1.98
Maximum air gap magnetic density	0.87	0.89	2.22

It can be seen from the data in Table 4 that the error of the magnetic density of the rotor yoke is 4.96%, which is relatively large compared with other parameters. This error is mainly caused by the rotor slot type and the length of the rotor core. These two parameters can be optimized again according to the actual operation requirements. In this paper, this optimization basically meets the design requirements.

The excitation control system of the distributed asynchronous condenser, in this paper, adds quantitative decoupling control which can adjust the slip through the change of voltage and current in the system. As shown in Figure 9, the slip rate changes from 0 to -0.05.

As can be seen from Figure 9, when the feedback parameters of the system reach the threshold in about 0.42s, the speed changes. At this time, the reactive power output of the condenser fluctuates slightly, but it soon recovers to stability. The speed changes rapidly from 3000 rpm to 2850 rpm, and energy conversion is bound to occur in this process. Figure 10 shows the kinetic energy and rotational speed diagram of the distributed asynchronous condenser under different slip rates.

As shown in Figure 9, through the reasonable setting of the control process, after the electrical parameters fed back in the grid exceed or decrease to a certain threshold, the asynchronous condenser control system will adjust the excitation frequency to realize the transformation of slip. The figure only shows the data with slip of -0.08 to +0.08. Within this range, this paper analyzes the influence of rotor kinetic energy corresponding to different slip rates. It can be found that when the slip rate decreases, the rotor kinetic energy will be released to the grid, meanwhile the active power and frequency of the system can be adjusted through control. Taking the process in Figure 9 as an example, when the slip rate changes from 0 to -0.05, the condenser can transmit 540kW equivalent active power to the system, which is about 2.7% of the rated capacity. Taking Figure 10 as an example, when the slip rate changes from 0.08 to -0.08, the asynchronous condenser can deliver about 1.6MW of equivalent

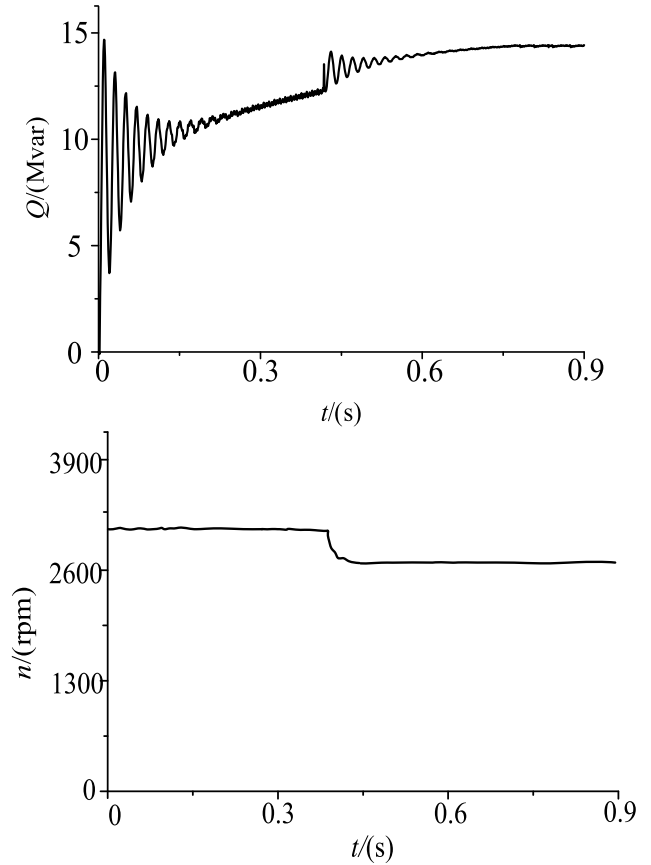


FIGURE 9. Reactive power(above) and speed(below) change.

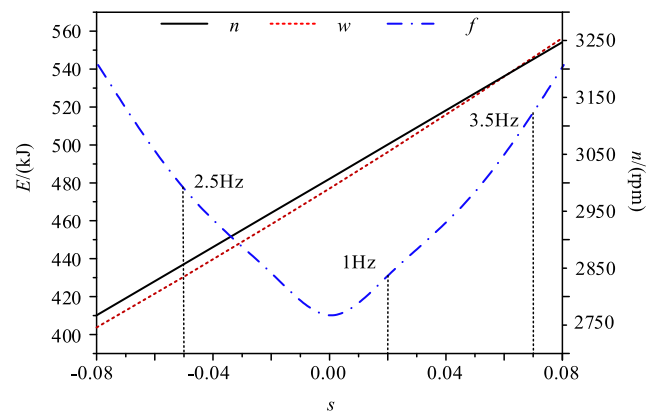


FIGURE 10. Different slip rates correspond to kinetic energy and speed.

active power to the system, about 8% of the rated capacity. In conclusion, the condenser has a certain supporting capacity for the inertia of the system when connected to the new energy system.

V. TRANSIENT CHARACTERISTICS

In order to verify the transient characteristics of distributed asynchronous condenser, this paper selects the most serious three-phase grounding short circuit and the most common single-phase grounding short circuit in power system, and sets different grounding resistors for analysis. According to

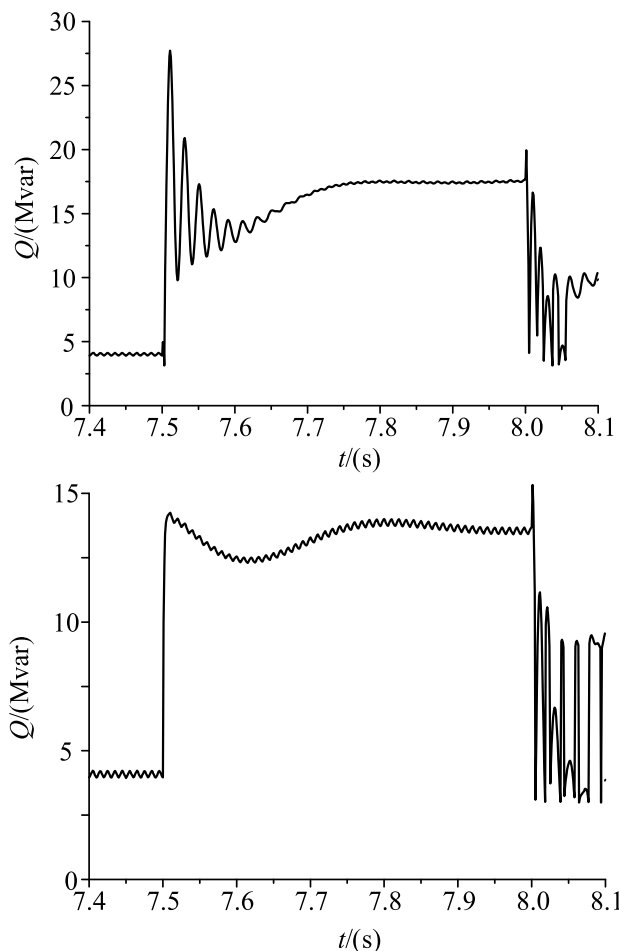


FIGURE 11. Reactive power output under three-phase short circuit fault when $R_k = 0.01\Omega$ (above) and $R_k = 100\Omega$ (below).

the current grounding protection and grounding conditions in the power system, the grounding resistance in small current grounding is generally more than 100Ω , and that in large current grounding is generally less than 0.1Ω . According to different voltage levels, fault conditions and grounding methods, the grounding resistance can even be $1\text{--}20\Omega$. Therefore, the grounding resistance set in this paper is 0.01Ω , 0.1Ω , 1Ω , 10Ω and 100Ω to simulate and analyze the mode.

Figure b in Figure 11 shows the effect of different grounding resistance on the reactive power output of the condenser. When the grounding resistance is large, the harmonic and unbalance parameters in the system are relatively small. The maximum reactive power output of the condenser can reach 14Mvar , and reach the fault stability period after 0.2s . At this time, the reactive power output is about 13Mvar . Figure a show that when the grounding resistance is small and a three-phase short circuit occurs in the system, the reactive power output of the distributed asynchronous condenser can reach 28Mvar in the ultra transient period and gradually decrease. Its reactive power oscillates around 14Mvar in the transient period. Different from the three-phase short circuit, the single-phase grounding short circuit is an asymmetric fault, and there will be negative sequence components in the

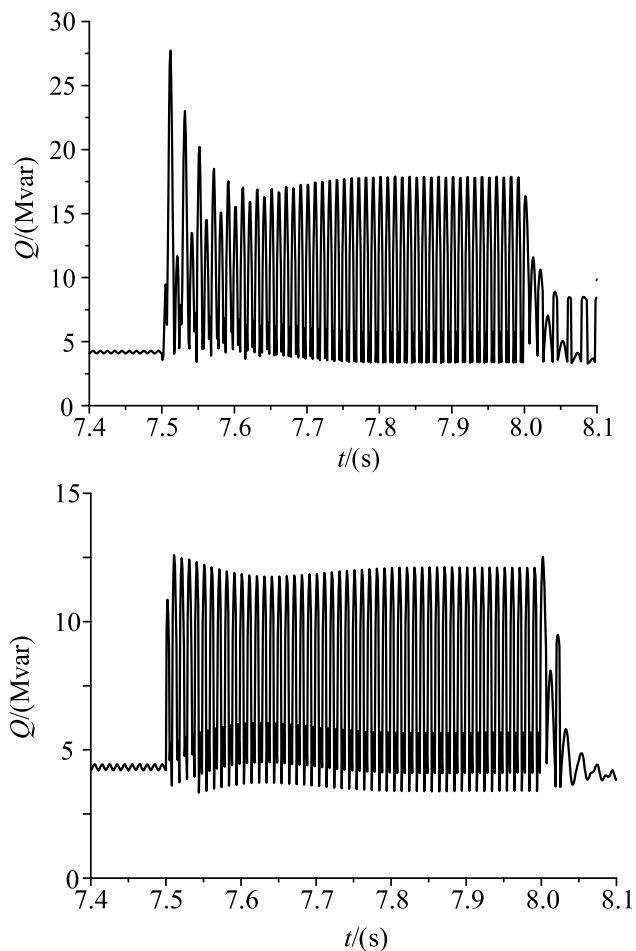


FIGURE 12. Reactive power output under single-phase grounding short-circuit fault when $R_k = 0.01\Omega$ (above) and $R_k = 100\Omega$ (below).

system, resulting in large oscillation amplitude of the reactive power output of the condenser. As shown in Figure 12, Figure a is the reactive power output when the grounding resistance is 0.01Ω , and Figure b is the reactive power output when the grounding resistance is 100Ω . It can be seen from the figure that the fault occurs at 7.5s and lasts for 0.5s . For the convenience of analysis, the default protection does not act. When the earthing resistance is small, the reactive power output of the regulator will oscillate at the instant of the fault and become stable slowly.

When the grounding resistance increases, the amplitude of the oscillation will be smaller and smaller. After the fault is removed, the condenser will resume stability in a shorter time. As shown in Figure 13, the change waveform of fault phase voltage in the system with and without distributed asynchronous condenser under single-phase grounding short-circuit fault, in which Figure a is the fault phase voltage waveform when the grounding resistance is 0.01Ω , and Figure b is the fault phase voltage waveform when the grounding resistance is 100Ω . It can be seen from the figure that the distributed asynchronous condenser can obviously raise the fault phase voltage of the system, and the maximum can be up to 2.5kV .

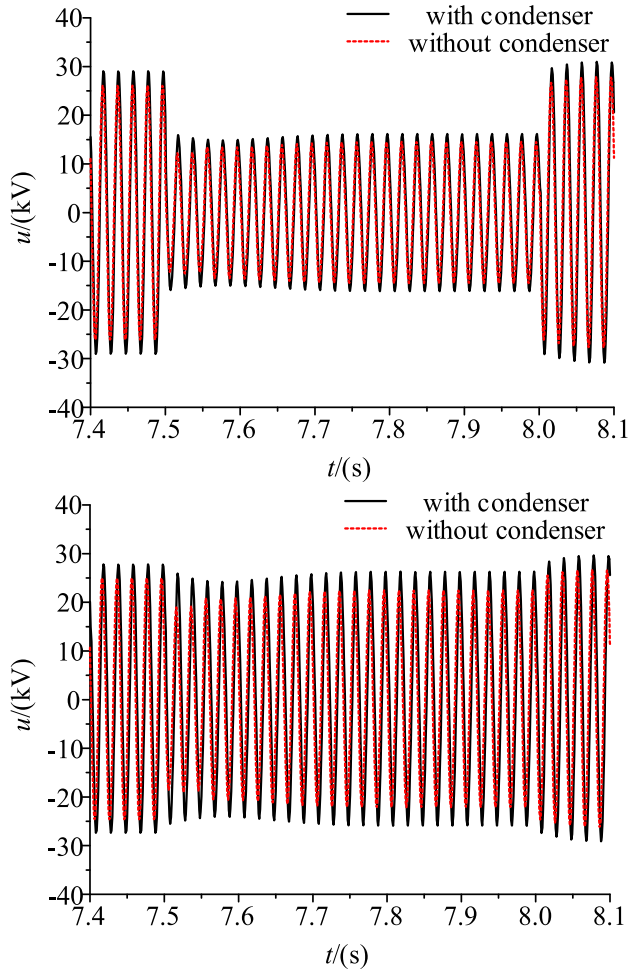


FIGURE 13. System voltage under single-phase grounding short-circuit fault when $R_k = 0.01 \Omega$ (above) and $R_k = 100 \Omega$ (below).

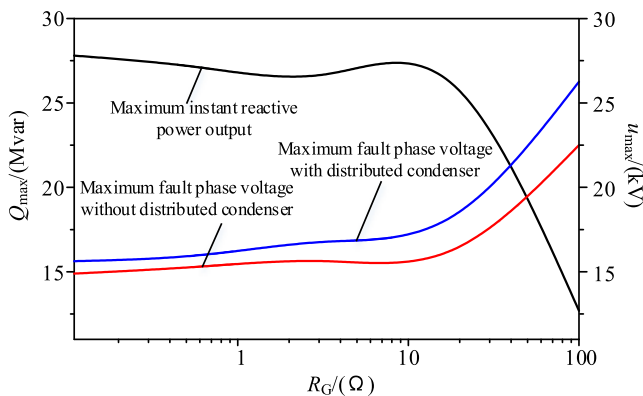


FIGURE 14. Comparison of different ground resistances.

In the current power system, due to the difference of different power supply voltage levels and specific configuration and installation environment, the size of grounding resistance is also different. Therefore, in order to verify the size of specific grounding resistance in the system suitable for distributed condenser, this paper selects the grounding resistance from 0.01Ω to 100Ω and carries out simulation analysis. The results are shown in Figure 14, It can be seen from the figure

that when the grounding resistance is less than 1Ω and near 10Ω , the instantaneous reactive power output of the motor is the largest.

VI. CONCLUSION

In this paper, the 20Mvar distributed asynchronous condenser is optimized, and the advantages and disadvantages of different excitation schemes are compared and analyzed to verify its output characteristics under different excitation frequencies. Then, through the established multi physical domain model, the transient characteristics of the distributed asynchronous condenser under different working conditions are analyzed. The main conclusions of this paper are as follows:

1) In order to improve the inertia and reduce the main reactance, an optimization process suitable for distributed asynchronous condenser is proposed in this paper. Taking the main reactance as an example, the effects of different air gap length and iron core length on the main reactance are analyzed. The results show that the main reactance is most sensitive to the air gap length, so the air gap length should be adjusted first in the subsequent optimization process by analyzing the influence of rotor kinetic energy corresponding to different slip rates. It is concluded that the condenser connected to the new energy system has a certain supporting capacity for the inertia of the system.

2) In this paper, five different synchronous excitation schemes are compared and analyzed. The weighted comparison of different parameters of different schemes is carried out by simplified analytic hierarchy process. The results show that three-phase overlapping excitation is the most suitable for distributed asynchronous condenser. After that, by analyzing the influence of rotor kinetic energy corresponding to different slip rates, it is concluded that the condenser connected to the new energy system has a certain supporting capacity for the inertia of the system. In the process of slip rate from 0.08 to -0.08 , it can output equivalent active power to the system of 1.6MW, which is about 8% of the rated capacity of the distributed asynchronous condenser, which shows that it has certain frequency modulation ability for the system.

3) In this paper, a multi physical domain joint simulation model is established, and the transient characteristics of the condenser under different fault conditions and different grounding resistance are analyzed. The results show that the distributed asynchronous condenser has a unique transient reactive power regulation ability in case of fault, and can quickly adjust the voltage level in the system.

The research results can provide theoretical basis and technical support for further parameter calculation and reasonable selection of grid connected operation. The distributed asynchronous condenser can adjust the system inertia according to further excitation control.

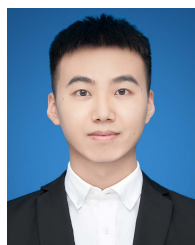
REFERENCES

[1] X. Ding, Y. Qiao, X. Z. Lu, Y. Min, and K. Bai, "Quantitative analysis of the influence of high proportion wind power on power system frequency modulation index," *Power Syst. Autom.*, vol. 38, no. 14, pp. 1–8, Jul. 2014.

- [2] Y. Li and J. X. Hu, "Influence of the spirit of 'carbon peak and carbon neutralization' on the development of China's power industry," *Public Electr.*, vol. 36, no. 3, pp. 10–11, Mar. 2021.
- [3] J. H. Gu, J. P. Liu, and H. Jiang, "Influence of wind power access on system frequency and overview of wind power frequency modulation technology," *Mod. Power*, vol. 32, no. 1, pp. 46–51, Feb. 2015.
- [4] S. Q. Zhou, Q. Wang, X. Lu, Y. Q. Hao, D. L. Liu, and Y. L. Ni, "Transient stability analysis of power system with large-scale wind farm," *Sichuan Electr. Power Technol.*, vol. 39, no. 5, pp. 9–13 and 25, Oct. 2016.
- [5] Y. Ye, Y. Qiao, and Z. Lu, "Revolution of frequency regulation in the converter-dominated power system," *Renew. Sustain. Energy Rev.*, vol. 111, pp. 145–156, Sep. 2019.
- [6] J. Ma, Y. Qiu, Y. Li, W. Zhang, Z. Song, and J. S. Thorp, "Research on the impact of DFIG virtual inertia control on power system small-signal stability considering the phase-locked loop," *IEEE Trans. Power Syst.*, vol. 32, no. 3, pp. 2094–2105, May 2017.
- [7] V. A. V. Mohanan, I. M. Y. Mareels, R. J. Evans, and R. R. Kolluri, "Stabilising influence of a synchronous condenser in low inertia networks," *IET Gener., Transmiss. Distrib.*, vol. 14, no. 17, pp. 3582–3593, Sep. 2020.
- [8] Y. Fu, Y. Wang, X. Zhang, and Y. Luo, "Analysis and integrated control of inertia and primary frequency regulation for variable speed wind turbines," *Chin. J. Electr. Eng.*, vol. 34, no. 27, pp. 4706–4716, Sep. 2014.
- [9] T. V. Van, K. Visscher, J. Diaz, V. Karapanos, A. Woyte, M. Albu, J. Bozelie, T. Loix, and D. Federenciu, "Virtual synchronous generator: An element of future grids," in *Proc. IEEE PES Innov. Smart Grid Technol. Conf. Eur. (ISGT Europe)*, Gothenberg, Sweden, Oct. 2010, pp. 1–7, doi: 10.1109/ISGTEUROPE.2010.5638946.
- [10] Z. Lu, W. Sheng, H. Liu, L. Sun, and M. Wu, "Application and challenge of virtual synchronous machine technology in power system," *Chin. J. Electr. Eng.*, vol. 37, no. 2, pp. 349–360, Nov. 2017.
- [11] Z. Xie, H. Meng, X. Zhang, and W. X. Jin, "Virtual synchronous control strategy of doubly fed wind turbine based on stator virtual impedance," *Power Syst. Autom.*, vol. 42, no. 9, pp. 157–163 and 187, May 2018.
- [12] J. Driesen and K. Visscher, "Virtual synchronous generators," in *Proc. IEEE Power Energy Soc. Gen. Meeting Convers. Del. Electr. Energy 21st Century*, Pittsburgh, PA, USA, Jul. 2008, pp. 1–3, doi: 10.1109/PES.2008.4596800.
- [13] X. Dai, "Research on microgrid control based on power electronic transformer grid connected device," Hangzhou Univ. Electron. Sci. Technol., School Electron. Information, Hangzhou, Tech. Rep., Dec. 2014.
- [14] P. Yang, X. Dong, Y. Li, L. Kuang, J. Zhang, B. He, and Y. Wang, "Research on primary frequency regulation control strategy of wind-thermal power coordination," *IEEE Access*, vol. 7, pp. 144766–144776, 2019.
- [15] D. S. Kumar, P. Lau, A. Sharma, A. Khambadkone, and D. Srinivasan, "Improvement of transient response in grid-tied photovoltaic systems using virtual inertia," *IET Smart Grid*, vol. 4, no. 1, pp. 1–14, Sep. 2021.
- [16] W. Cao, T. Zhang, Y. S. Fu, B. L. Yao, and S. Y. Chen, "Research and application of synchronous condenser to enhance power system inertia and improve frequency response," *Power Syst. Autom.*, vol. 44, no. 3, pp. 1–10, Mar. 2020.
- [17] Y. Zhou, H. Sun, X. Wang, S. Xu, B. Zhao, D. Guo, and C. Wang, "Suppressing overvoltage by synchronous condenser based on multiple renewable energy stations short circuit ratio (MRSCR)," in *Proc. IEEE 5th Conf. Energy Internet Energy Syst. Integr. (EI2)*, Oct. 2021, pp. 918–923, doi: 10.1109/EI252483.2021.9713629.
- [18] China Dongfang Electric Group Co., Ltd, "The first 50 Mvar salient pole condenser in China was put into operation," *Electr. World*, vol. 62, no. 10, p. 56, May 2021.
- [19] H. H. Zhang, Q. L. Xing, W. X. Yan, and Z. Q. Mi, "Summary of asynchronous synchronous generator," *North China Electr. Power*, vol. 7, no. 4, pp. 83–104, Oct. 2000.
- [20] A. C. Ferreira, L. M. Souza, and E. H. Watanabe, "Improving power quality with a variable speed synchronous condenser," in *Proc. Int. Conf. Power Electron. Mach. Drives*, 2002, pp. 456–461.
- [21] G. R. Xu, P. Y. Hu, L. W. Li, L. Y. Luo, and F. X. Liu, "Variation law of synchronous reactance of double shaft excitation synchronous motor with operating conditions," *Trans. China Electrotech. Soc.*, vol. 35, no. 2, pp. 236–245, Jan. 2020.
- [22] S. C. Yang, Y. Liao, and H. Li, *Asynchronous Synchronous Generator*. Beijing, China: Science Press, 2009, pp. 1–3.
- [23] Y. J. Wan, L. W. Xiu, J. R. Chen, L. L. Wang, S. Li, and N. Liu, "Simulation analysis of starting characteristics of large capacity asynchronous motor," *China Meas. Test*, vol. 40, no. 6, pp. 132–136, Nov. 2020.
- [24] J. Y. Chen, H. H. Yu, and X. T. Yang, "Design of multi parallel branch winding of 300 Mvar condenser," *Large Electr. Mach. Hydraulic Turbine*, vol. 2020, no. 4, pp. 15–18, Jul. 2020.



ZHIPENG LIU was born in Heilongjiang, China, in 1989. He received the M.S. degree in electrical engineering from the Harbin University of Science and Technology (HUST), in 2015. Currently, he is an Excellent Electrical Engineer with many achievements. His research interests include the machine network coordination technology, new energy power generation technology, and secondary system control and fault monitoring.



HAIBING QI was born in Heilongjiang, China, in 1998. He received the B.Eng. degree in electrical engineering from the Harbin University of Science and Technology (HUST), Harbin, China, in 2019. Currently, he is a Graduate Student in power system and automation with HUST. His research interests include the power system operation and protection, new energy power generation technology, and motor design.



MINGYU XU was born in 1983. He received the B.Sc. and M.Sc. degrees from North China Electric Power University, China, in 2005 and 2009, respectively. He is currently a Senior Engineer with the Heilongjiang Electric Power Research Institute, China. His research interests include the relay protection of secondary systems and equipment status assessment.



XINGYUAN JIANG was born in Heilongjiang, China, in 1995. He received the B.Eng. degree in electrical engineering from the Harbin University of Science and Technology (HUST), Harbin, China, in 2018. Currently, he is a Graduate Student in power system and automation with HUST. His research interests include power system stability analysis, new motor control, and new energy power generation systems.



YANLING LV was born in Heilongjiang, China, in 1975. She received the Ph.D. degree in electrical engineering from the Harbin University of Science and Technology (HUST), Harbin, China, in 2010, respectively. Currently, she is a Professor with HUST. Her research interests include the operation and protection of large generators, generators and its system operation analyses, power system fault, and protection analyses.